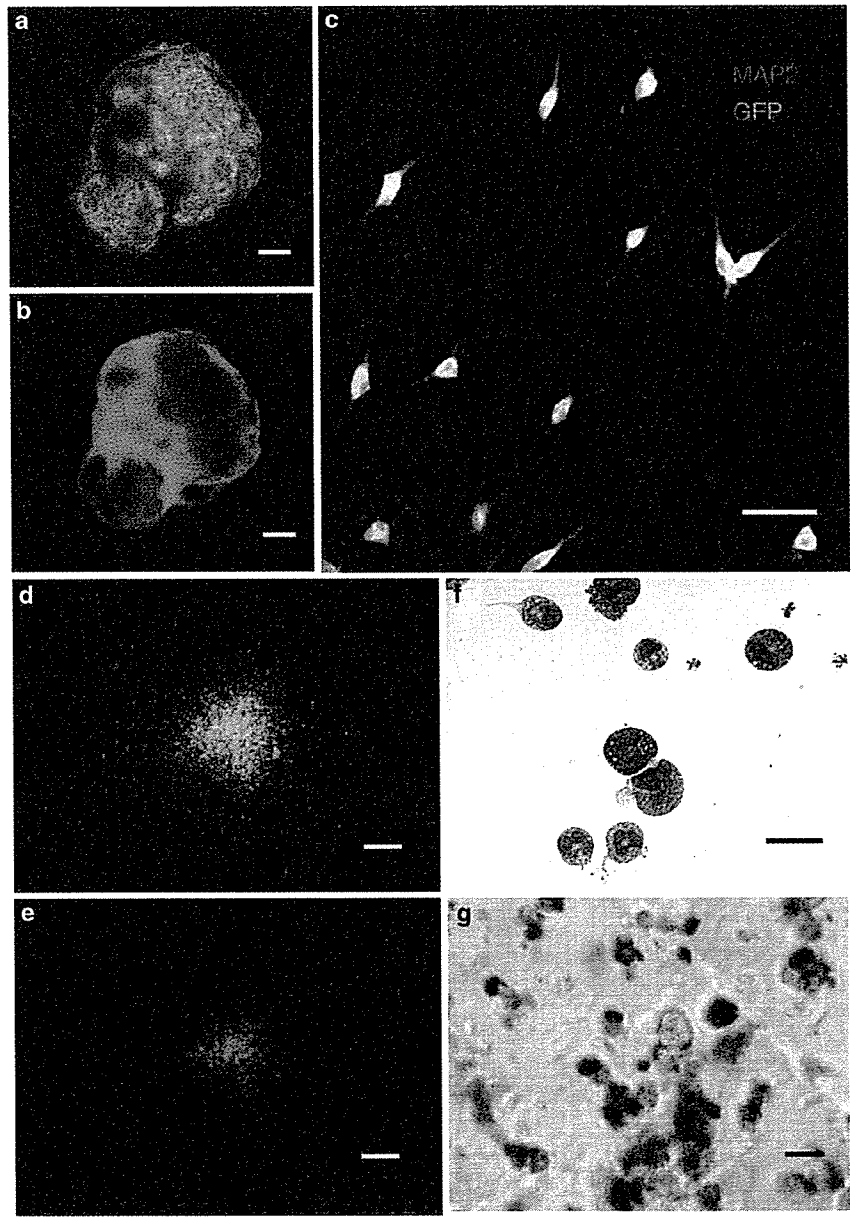

Figure 5 Stable transgene expression during differentiation. A day-20 cystic embryoid body was observed under a fluorescent phase-contrast microscope, confirming that the embryoid body was fluorescing ((a), bright field; (b), dark field). After infection with the SeV vector, fluorescent cynomolgus ES cells differentiated into neural cells. Double immunostaining with anti-GFP (green) and ant-MAP-2 (red) confirmed that differentiated neural cells expressed GFP (c). Yellow cells indicate GFP-expressing neurons. SeV-infected, fluorescent cynomolgus ES cells also differentiated into fluorescent hematopoietic cells. A clonogenic hematopoietic colony was fluorescing ((d) bright field; (e), dark field). A cytospin specimen of hematopoietic colony cells (Wright–Giemsa staining) showed that the cells were mature granulocytes (f). The infected ES cell-derived, fluorescent neutrophils were positive for NBT (stained in black (g)). Bar = 100 μm (a, b, g); 50 μm (c, f); 500 μm (d, e).

viral particles in infected cells were quantified by a hemagglutination assay as described previously.[25]

An adenovirus serotype 5-based vector carrying the GFP gene was constructed as reported.[26] It contained the cytomegalovirus (CMV) promoter, simian virus (SV)-40 intron, and SV-40 polyadenylation signal. An AAV serotype 2-based vector expressing the GFP gene under the control of the chicken β-actin promoter with the CMV immediate-early enhancer (a gift from Dr J Miyazaki) was prepared as described previously.[27] Gene transfer experiments were performed using 3.4×10^2 genome copies (g.c.)/cell of the adenoviral vector or 2.4×10^4 g.c./cell of the AAV vector. The period of exposure was 48 h.

Flow cytometry

GFP and SSEA-4 expression was analyzed on a FACScan (Becton Dickinson, Franklin Lakes, NJ, USA) using the

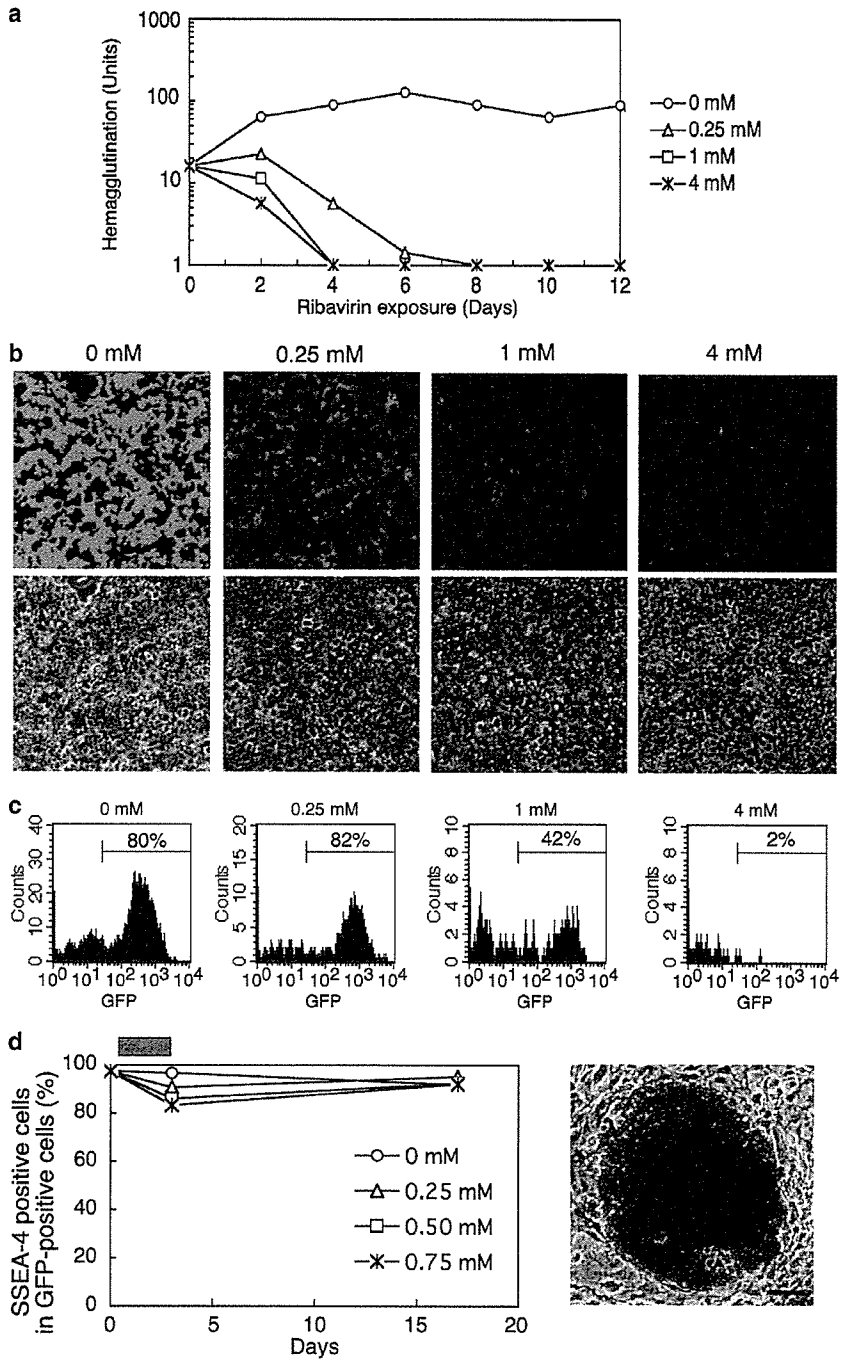

Figure 6 Ribavirin-regulated transgene expression. (a) A rhesus kidney cell line (LLC-MK2) was infected with the SeV vector at 3 TU/cell. Ribavirin was started at various concentrations on day 2 after the infection. The formation of viral particles in the infected LLC-MK2 cells was examined by the hemagglutination assay. (b) The ribavirin-treated LLC-MK2 cells were observed under a fluorescent microscope after an 8-day exposure of ribavirin (upper, dark field; lower, bright field). (c) Ribavirin was added at various concentrations to the SeV-infected, fluorescent cynomolgus ES cells. The GFP expression was assessed by flow cytometry after a 3-day exposure of ribavirin. (d) The fractions of SSEA-4-positive ES cells were assessed by flow cytometry with anti-SSEA-4 before and after a 3-day exposure of ribavirin and are shown as a function of time (days) in the left panel. A gray bar indicates ribavirin treatment. ES cells were stained for alkaline phosphatase (in red) at day 21 after a 3-day exposure of 0.75 mM ribavirin and are shown in the right panel. Bar = 100 μm.

CellQuest software (Becton Dickinson). For SSEA-4 staining, cells were incubated with a primary antibody, anti-SSEA-4 (MC-813-70; Chemicon, Temecula, CA, USA), and then a secondary antibody, PE-conjugated F(ab')2 fragment of rabbit anti-mouse immunoglobulins (DakoCytomation, Glostrup, Denmark). Cocultured BALB/c feeder cells could be distinguished from cynomolgus ES cells by using PE-conjugated anti-mouse

H-2d (SF1-1.1; PharMingen, San Diego, CA, USA), which does not react to cynomolgus cells but does react to BALB/c cells.

Teratoma formation

Cynomolgus ES cells (approximately 10^6 cells per site) were injected subcutaneously into the hind leg of 6- to 8-week-old nonobese diabetic/severe combined immunodeficient mice (Jackson Laboratory, Bar Harbor, ME, USA). The resulting tumors (usually 9–12 weeks after the injection) were dissected and fixed in 4% paraformaldehyde. For histological analysis, samples from the tumors were embedded in paraffin and stained with hematoxylin and eosin. To observe GFP fluorescence, samples were embedded in OTC compound (Sakura, Zoeterwoude, Netherlands), frozen, sectioned, and examined under a fluorescence microscope.

Hematopoietic differentiation

The mouse bone marrow stromal cell line OP9 was maintained in α-modified minimum essential medium (Invitrogen) supplemented with 20% FCS as described previously.[28] For induction of hematopoietic differentiation, ES cells were seeded onto a mitomycin C-treated confluent OP9 cell layer in six-well plates. Medium to support the differentiation was described elsewhere.[29] Cells at day 18 were placed in Methocult GF+ media (StemCell Technologies, Vancouver, Canada) at 1×10^4 and 1×10^5 cells per plate and clonogenic hematopoietic colonies were produced. After 14 days, individual colonies were removed and spun onto glass slides. Cells were stained with the Wright–Giemsa method. The nitro blue tetrazolium (NBT, Sigma) reduction test was performed on the cells as a granulocyte functional assay according to a previously described method.[30]

Neural differentiation

The induction of neural differentiation was carried out as described previously.[31] Day-4 embryoid bodies were plated onto tissue culture dishes and nestin-positive cells were selected in DMEM/F12 medium supplemented with 5 μg/ml of insulin (Sigma), 50 μg/ml of transferrin (Sigma), 30 nM selenium chloride (Sigma), and 5 μg/ml of fibronectin (Sigma) for 5 days. Cells were then trypsinized and plated in polyornithine-coated dishes (15 μg/ml) and expanded in N2 medium[32] supplemented with 1 μg/ml of laminin (Sigma) and 10 μg/ml of basic fibroblast growth factor (bFGF; Roche, Basel, Switzerland) for 6 days. Differentiation was induced by removal of bFGF. To confirm the neural differentiation, cells were stained with anti-human MAP-2. Briefly, cells were fixed in 4% paraformaldehyde in PBS and incubated with anti-human MAP-2 (HM-2; Sigma; diluted 1:4000) and then by Alexa Fluor 594-labeled antibody (diluted 1:500; Molecular Probe, Eugene, OR, USA). The samples were examined under a fluorescence microscope.

DNA-PCR

DNA-PCR for the SeV genome and GFP sequences was carried out as follows. DNA was extracted using the QIAamp DNA mini kits (Qiagen, Hilden, Germany) and 250 ng was used for each PCR with ExTaq (Takara, Shiga, Japan). Amplification conditions were 30 cycles of 94°C for 1 min, a variable annealing temperature (noted below) for 1 min, and 72°C for 1 min. The amplified products were run on 2% agarose gel and visualized by ethidium bromide staining. Primer sequences, annealing temperatures and product sizes were as follows: the SeV vector genome sequence: 5′-AGA GAA CAA GAC TAA GGC TAC C-3′ and 5′-ACC TTG ACA ATC CTG ATG TGG-3′ (55°C, 580 bp); the GFP sequence: 5′-CGT CCA GGA GCG CAC CAT CTT C-3′ and 5′-GGT CTT TGC TCA GGG CGG ACT-3′ (60°C, 356 bp). the cynomolgus β-actin sequence: 5′-CAT TGT CAT GGA CTC TGG CGA CGG-3′ and 5′-CAT CTC CTG CTC GAA GTC TAG GGC-3′ (60°C, 234 bp).

RNA-PCR

RNA-PCR for the SeV RNA genomic sequence was carried out as follows. Total RNA was extracted using RNA STAT-60 (Tel-Test, Friendswood, TX, USA). Reverse transcription was conducted by using Taqman reverse transcription reagents (Applied Biosystems, Foster City, CA, USA). The product (250 ng) after the reverse transcription was used for the subsequent PCR as described above.

Acknowledgements

Cynomolgus ES cells were provided by Norio Nakatsuji (Kyoto University, Kyoto, Japan), Yasushi Kondo (Tanabe Seiyaku Co. Ltd, Osaka, Japan), and Ryuzo Torii (Shiga University of Medical Science, Shiga, Japan). OP9 cells were provided by Toru Nakano (Osaka University, Osaka, Japan). We thank Yujiro Tanaka and Takayuki Asano for cultivating cynomolgus ES cells and Takeshi Hara for conducting NBT tests. We also thank Natsuko Kurosawa for technical assistance.

References

1 Thomson JA *et al.* Embryonic stem cell lines derived from human blastocysts. *Science* 1998; **282**: 1145–1147.
2 Reubinoff BE *et al.* Embryonic stem cell lines from human blastocysts: somatic differentiation *in vitro*. *Nat Biotechnol* 2000; **18**: 399–404.
3 Asano T *et al.* Highly Efficient gene transfer into primate embryonic stem cells with a simian lentivirus vector. *Mol Ther* 2002; **6**: 162–168.
4 Ma Y *et al.* High-level sustained transgene expression in human embryonic stem cells using lentiviral vectors. *Stem Cells* 2003; **21**: 111–117.
5 Gropp M *et al.* Stable genetic modification of human embryonic stem cells by lentiviral vectors. *Mol Ther* 2003; **7**: 281–287.
6 Li HO *et al.* A cytoplasmic RNA vector derived from nontransmissible Sendai virus with efficient gene transfer and expression. *J Virol* 2000; **74**: 6564–6569.
7 Yonemitsu Y *et al.* Efficient gene transfer to airway epithelium using recombinant Sendai virus. *Nat Biotechnol* 2000; **18**: 970–973.
8 Masaki I *et al.* Recombinant Sendai virus-mediated gene transfer to vasculature: a new class of efficient gene transfer vector to the vascular system. *FASEB J* 2001; **15**: 1294–1296.
9 Shiotani A *et al.* Skeletal muscle regeneration after insulin-like growth factor I gene transfer by recombinant Sendai virus vector. *Gene Therapy* 2001; **8**: 1043–1050.
10 Yamashita A *et al.* Fibroblast growth factor-2 determines severity of joint disease in adjuvant-induced arthritis in rats. *J Immunol* 2002; **168**: 450–457.

11 Ikeda Y *et al.* Recombinant Sendai virus-mediated gene transfer into adult rat retinal tissue: efficient gene transfer by brief exposure. *Exp Eye Res* 2002; **75**: 39–48.
12 Jin CH *et al.* Recombinant Sendai virus provides a highly efficient gene transfer into human cord blood-derived hematopoietic stem cells. *Gene Therapy* 2003; **10**: 272–277.
13 Crotty S *et al.* The broad-spectrum antiviral ribonucleoside ribavirin is an RNA virus mutagen. *Nat Med* 2000; **6**: 1375–1379.
14 Vo NV, Young KC, Lai MM. Mutagenic and inhibitory effects of ribavirin on hepatitis C virus RNA polymerase. *Biochemistry* 2003; **42**: 10462–10471.
15 McHutchison JG *et al.* Interferon alfa-2b alone or in combination with ribavirin as initial treatment for chronic hepatitis C. Hepatitis Interventional Therapy Group. *N Engl J Med* 1998; **339**: 1485–1492.
16 Davis GL *et al.* Interferon alfa-2b alone or in combination with ribavirin for the treatment of relapse of chronic hepatitis C. International Hepatitis Interventional Therapy Group. *N Engl J Med* 1998; **339**: 1493–1499.
17 McCormick JB *et al.* Lassa fever. Effective therapy with ribavirin. *N Engl J Med* 1986; **314**: 20–26.
18 Suemori H *et al.* Establishment of embryonic stem cell lines from cynomolgus monkey blastocysts produced by IVF or ICSI. *Dev Dyn* 2001; **222**: 273–279.
19 Spann KM, Collins PL, Teng MN. Genetic recombination during coinfection of two mutants of human respiratory syncytial virus. *J Virol* 2003; **77**: 11201–11211.
20 Tozawa H *et al.* Neutralizing activity of the antibodies against two kinds of envelope glycoproteins of Sendai virus. *Arch Virol* 1986; **91**: 145–161.
21 Tashiro M, Tobita K, Seto JT, Rott R. Comparison of protective effects of serum antibody on respiratory and systemic infection of Sendai virus in mice. *Arch Virol* 1989; **107**: 85–96.
22 Inoue M *et al.* Nontransmissible virus-like particle formation by F-deficient Sendai virus is temperature sensitive and reduced by mutations in M and HN proteins. *J Virol* 2003; **77** 3238–3246.
23 Inoue M *et al.* A new Sendai virus vector deficient in the matrix gene does not form virus particles and shows extensive cell-to-cell spreading. *J Virol* 2003; **77**: 6419–6429.
24 Inoue M *et al.* Recombinant Sendai virus vectors deleted in both the matrix and the fusion genes: efficient gene transfer with preferable properties. *J Gene Med*, published online 5 May 2004 doi:10.1002/jgm.597.
25 Kato A *et al.* Initiation of Sendai virus multiplication from transfected cDNA or RNA with negative or positive sense. *Genes Cells* 1996; **1**: 569–579.
26 Okada T *et al.* Efficient directional cloning of recombinant adenovirus vectors using DNA–protein complex. *Nucleic Acids Res* 1998; **26**: 1947–1950.
27 Okada T *et al.* Adeno-associated viral vector-mediated gene therapy of ischemia-induced neuronal death. *Methods Enzymol* 2002; **346**: 378–393.
28 Nakano T, Kodama H, Honjo T. Generation of lympho-hematopoietic cells from embryonic stem cells in culture *Science* 1994; **265**: 1098–1101.
29 Li F *et al.* Bone morphogenetic protein 4 induces efficient hematopoietic differentiation of rhesus monkey embryonic stem cells *in vitro*. *Blood* 2001; **98**: 335–342.
30 Sekhsaria S *et al.* Peripheral blood progenitors as a target for genetic correction of $p47^{phox}$-deficient chronic granulomatous disease. *Proc Natl Acad Sci USA* 1993; **90**: 7446–7450.
31 Lee SH *et al.* Efficient generation of midbrain and hindbrain neurons from mouse embryonic stem cells. *Nat Biotechnol* 2000; **18**: 675–679.
32 Johe KK *et al.* Single factors direct the differentiation of stem cells from the fetal and adult central nervous system. *Genes Dev* 1996; **10**: 3129–3140.
33 Takada T *et al.* Monkey embryonic stem cell lines expressing green fluorescent protein. *Cell Transplant* 2002; **11**: 631–635.

Clinical Study

Chemotherapy

Chemotherapy 2005;51:120–125
DOI: 10.1159/000085619

Received: May 15, 2004
Accepted after revision: November 19, 2004
Published online: May 9, 2005

A Phase II Study of Docetaxel and Infusional Cisplatin in Advanced Non-Small-Cell Lung Cancer

Kiyoshi Mori Yukari Kamiyama Tetsuro Kondo Yasuhiko Kano
Tetsuro Kodama

Department of Thoracic Diseases, Tochigi Cancer Center, Yonan, Utsunomiya, Japan

Key Words
Non-small-cell lung cancer · Chemotherapy · Cisplatin · Docetaxel · Infusion, continuous

Abstract
Background: To evaluate the efficacy and safety of combination chemotherapy of cisplatin (5-day continuous infusion) and docetaxel for the treatment of previously untreated patients with advanced non-small-cell lung cancer (NSCLC). ***Materials and Methods:*** Eligible patients had an ECOG performance status of 0–2 with measurable NSCLC. Patients received continuous infusion cisplatin 20 mg/m^2/day on 5 days and bolus docetaxel 60 mg/m^2/day (day 1; PiD therapy) at a 4-week interval. ***Results:*** Forty-three patients were enrolled. The mean number of cycles administered per patient was 2, and ranged from 1 to 4. The response rate was 49% (95% confidence interval, 33.9–63.8%). The median survival time was 47 weeks and the 1-year survival rate was 47%. The major toxic effects were grade 3 or 4, neutropenia (88%), leukopenia (81%), thrombocytopenia (14%) and anemia (42%). There were no treatment-related deaths. ***Conclusion:*** PiD therapy was a well-tolerated and active regimen for patients with advanced NSCLC. The major toxicity was neutropenia.

Introduction

Unresectable non-small-cell lung cancer (NSCLC) is known to have an extremely poor prognosis, and its standard treatment remains to be established. The most common chemotherapy for NSCLC is a combination treatment consisting of 2 or 3 drugs including cisplatin (CDDP) as a key drug. The combination treatments have response rates of 30–50%, and have been proven to prolong survival time in clinical stages III [1] and IV [2, 3]; however, the response is only limited.

In recent years, new anticancer drugs have been developed and used for the treatment of NSCLC. Docetaxel is a new hemisynthetic anticancer agent originating from its precursor, 10-deacytylbaccatin III, extracted from the needle leaves of the European yew tree, *Taxus baccata* L. Docetaxel affects microtubules, and shows its cytotoxicity by prematurely stabilizing mitotic microtubules. In phase II clinical studies for the treatment of NSCLC carried out in Europe and the USA, docetaxel showed a response rate of about 30% in previously untreated patients with a better survival time [4, 5]. A major side effect of docetaxel is dose-dependent edema that is proportional to bone marrow suppression. Since hypersensitivity is particularly limiting, it is worth noting that docetaxel can be given by intravenous infusion in a short period of time without any pretreatment.

KARGER
Fax +41 61 306 12 34
E-Mail karger@karger.ch
www.karger.com

0009–3157/05/0513–0120$22.00/0

Accessible online at:
www.karger.com/che

Kiyoshi Mori
Department of Thoracic Diseases, Tochigi Cancer Center
4-9-13, Yonan
Utsunomiya, Tochigi 320-0834 (Japan)
Tel. +81 28 658 5151, Fax +81 28 658 5669, E-Mail kmori@tcc.pref.tochigi.jp

In the Japan phase I study, dose-limiting toxicity of docetaxel was found to be leukopenia (neutropenia), and its recommended dose was set at 60 mg/m^2 [6]. In the multicenter phase II clinical study for the treatment of NSCLC carried out in Japan, a response rate of 19% was shown in untreated patients with predominant toxicities of leukopenia and neutropenia [7].

Currently, cisplatin is the active agent for treating NSCLC, and combination chemotherapy consisting of 2 or 3 drugs based on CDDP is a major strategy [8]. CDDP can be administered by short-term intravenous infusion, a divided dosage method, continuous administration, and other methods [9, 10]. CDDP cytotoxicity is enhanced by prolonged exposure to low doses of this drug in in vitro studies [11, 12]. Belliveau et al. [13] reported that the area under the concentration-time curve (AUC) achieved for non-protein-bound CDDP was twice as high after 5-day continuous infusion than that observed when an equivalent dose of CDDP was given by short-term bolus infusion. These findings suggest that continuous infusion of CDDP might improve the therapeutic efficacy as compared with that resulting from conventional short-term bolus infusion. However, compared with short-term intravenous infusion, 5-day continuous infusion makes inpatient hospitalization for at least 5 days necessary, and the duration of confinement for the purpose of infusion is lengthy and therefore onerous for the patient. The efficacy and safety of a continuous infusion lasting 5 days (24 h a day) were confirmed in our facility and some other facilities [10, 14–16]. In addition, combination chemotherapy of infusional CDDP with vindesine or CPT-11 was found to have high response rates in treating NSCLC [17, 18].

Cisplatin and docetaxel show nonsynergistic and additive effects in vitro, no cross-resistance and have a relatively nonoverlapping toxicity profile [19]. Therefore, the development of docetaxel in combination with cisplatin is warranted. We conducted a phase II study of docetaxel and infusional cisplatin, in patients with previously untreated advanced NSCLC, and evaluated antitumor activity and the safety of this therapy.

Patients and Methods

Patient Selection

All patients with histologically or cytologically confirmed advanced NSCLC were eligible for this phase II trial. The subjects of this study were patients in clinical stage IV or in stage III with unresectable disease or in whom radiotherapy with curative intent is not possible. Patients with unresectable disease or in whom radiotherapy with curative intent is not possible include those with pleural effusion and dissemination, those with intrapulmonary metastasis within the ipsilateral lobe, those in whom the irradiation field exceeds one half of one lung, those with metastasis to the contralateral hilar lymph nodes, and those with reduced lung function. None of the patients had received prior therapy. Other eligibility criteria included an expected survival of 12 weeks, age $\leq$75 years, Eastern Cooperative Oncology Group performance score of 0–2, measurable lesions, adequate hematological function (WBC $\geq$4,000/mm^3, platelet count $\geq$100,000/mm^3, hemoglobin $\geq$10 g/dl), renal function (serum creatinine $\leq$1.5 mg/dl, creatinine clearance $\geq$60 ml/min), and hepatic function (total serum bilirubin $\leq$1.5 mg/dl, glutamic oxaloacetic transaminase and glutamic pyruvic transaminase less than twice the normal range). The ethical committee of the Tochigi Cancer Center approved the protocols. Written informed consent was obtained in every case stating that the patient was aware of the investigational nature of this treatment regimen. Pretreatment evaluation included medical history, physical examination, complete blood count, bone marrow examination, serum biochemical analyses, chest roentgenogram, electrocardiogram, and urinalysis. All patients underwent a radionuclide bone scan, and computerized tomography of the brain, thorax and abdomen. Complete blood count, biochemical tests, serum electrolytes, urinalysis, and chest roentgenograms were obtained weekly during this phase II trial. Tests of measurable disease parameters such as computerized tomography were repeated every 4 weeks. Staging was according to the 4th edition of the UICC TNM classification.

Treatment

All patients were admitted to the Tochigi Cancer Center Hospital during this trial. The anticancer drug regimen consisted of a combined administration of docetaxel plus infusional cisplatin. Docetaxel was supplied, in concentrated form, in a sterile vial that contained 80 mg of the drug in 2 ml of polysorbate 80. Docetaxel (Taxotere; Aventis) 60 mg/m^2 was diluted in 250 ml of 5% glucose, and was infused over a 1-hour period on day 1. Three hours after completion of the docetaxel infusion, 20 mg/m^2 of cisplatin was given daily for 5 days by continuous intravenous infusion. One third of the daily dose was administered every 8 h dissolved in 800 ml of physiological saline [14]. The course was repeated every 4 weeks. Antiemetic drugs used were granisetron (3 mg/body/day, bolus infusion for 5 days), metoclopramide (3 mg/kg/day, continuous infusion for 5 days), methylprednisolone (125 mg bolus infusion every 8 h, days 1–5), diphenhydramine (30 mg orally, days 1–7) and alprazolam (1.2 mg orally, days 1–7) [15, 16]. In the first course, no routine premedication was given for hypersensitivity reactions or fluid retention. The reason for this was that the incidence of these events was low at the dose of docetaxel (60 mg/m^2) administered in the present study [7]. However, if hypersensitivity reactions or fluid retention occurred, premedications such as corticosteroids or antiallergic agents were allowed in the subsequent courses. Recombinant human granulocyte colony-stimulating factor was administered when leukopenia/neutropenia of grade 4 occurred.

Patients were treated with at least two cycles of therapy unless disease progression or unacceptable toxicity was encountered or the patients did not wish to continue. Patients who experienced grade 4 leukopenia or neutropenia that lasted for 3 or more days, or who experienced grade 4 thrombocytopenia or reversible grade 2 neurotoxicity or grade 3 liver dysfunction, received reduced doses of

both docetaxel and cisplatin (75% of the previous dose) for the next cycle. Patients who experienced stomatitis of grade 3 or more or renal dysfunction of grade 2 or more received a reduced dose of cisplatin (75% of the previous dose) for the next cycle. If neurotoxicity of grade 3 or more occurred, treatment was stopped. Subsequent courses of chemotherapy were started after day 28 when the leukocyte count was 4,000/mm^3 or more, the neutrophil count was 2,000/mm^3 or more, the platelet count was 100,000/mm^3 or more, serum creatinine was less than the upper limit of the normal range, creatinine clearance was 60 ml/min or more, GOT and GPT were less than twice the upper limit of the normal range, and neurotoxicity was grade 1 or less. If these variables did not return to adequate levels by the first day of the next course of chemotherapy, treatment was withheld until full recovery. If more than 6 weeks passed from the time of the last treatment before these criteria were satisfied, the patient was taken off the study, but still included in the analysis. In the case of stable or progressive disease after two courses of treatment, subsequent therapy was left to the discretion of the physician in charge of the patient.

Assessment of Response to Treatment and Toxicity

The response to treatment was evaluated with WHO criteria. The criteria for response were as follows. Complete response was defined as the complete disappearance of all evidence of tumor for at least 4 weeks. Partial response was defined as a ≥ 50% reduction in the sum of the product of the two greatest perpendicular diameters of all indicator lesions for at least 4 weeks and no appearance of new lesions or progression of any lesion. Progressive disease was defined as a ≥ 25% increase in the tumor area or the appearance of new lesions. All other circumstances were classified as no change. Toxicity was graded according to the common toxicity criteria (version 2).

Statistical Analyses

The primary end point was the objective response rate. The duration of each response was defined as the number of days from the documentation of the response until tumor progression. Survival curves from registration until death were generated by the method of Kaplan and Meier. We chose a 40% response rate as a desirable target level, and a 20% response rate as undesirable. The study design had the power to detect a response of greater than 90%, with less than 5% error. Therefore, we needed 23 assessable patients in first stage and 20 in second stage, according to the mini-max design of Simon. We decided to stop the study if fewer than 5 patients responded in the first stage.

Results

Patient Characteristics

Forty-three patients were enrolled in this study from July 1997 to June 1999 and received 105 cycles of the regimen. Table 1 shows the patient characteristics. There were 14 women and 29 men with a median age of 61 years (range 34–75). One patient had stage IIIA, 7 patients stage IIIB, and 35 patients stage IV disease. In stage IIIA, 1 patient classified as c-T3N2M0 had lung cancer with a bulky tumor (10 cm), associated with extranodal and N2 involvement. Among the 7 stage IIIB patients, there were three T4 cases in which pleural effusion and pleural dissemination were present, two T4 cases of intrapulmonary metastasis in the ipsilateral lobe, and two T4N3 cases with mediastinal infiltration and supraclavicular fossa lymph node metastasis.

Table 1. Patient characteristics

Patients	43
Sex (M/F)	29/14
Age[1], years	61 (34–75)
Performance status: 0/1/2	9/30/4
Stage: IIIA/IIIB/IV	1/7/35
Histology: Ad/Sq/Other	27/14/2

Ad = Adenocarcinoma; Sq = squamous cell carcinoma.

[1]Value represents median with the range given in parentheses.

Treatments Administered

The mean number of cycles administered per patient was 2, and ranged from 1 to 4. In 99 of 105 cycles (94%), PiD was administered at 4-week intervals. In 5 of 6 cycles, in which cisplatin could not be administered at a 4-week interval, it was given a week later. As for the remaining cycle, it was administered 6 weeks later. The reason for the delay of the administration was the patient's request for 1 cycle and neutropenia in 5 cycles. Dosage was reduced in 7 cycles (7%). Reductions in dosage of docetaxel and cisplatin were made, respectively, in 6 cycles (6%) and 7 cycles (7%). The former reduction was made because 6 cycles showed neutropenia grade 4, and the latter reduction was made because 5 cycles showed neutropenia grade 4, and 1 cycle showed both neutropenia grade 4 and creatinine grade 3, and 1 cycle showed creatinine grade 2.

Response to Treatment and Survival

The response rate was 49% (95% confidence interval, CI, 33.9–63.8%); a complete response was observed in 1 and partial response in 20 patients (table 2). The median duration of the response was 39.2 weeks (range 5–147 weeks). The median survival time was 47 weeks (95% CI, 6–152 weeks) and the 1-year survival rate was 47% (fig. 1). Two patients are still alive.

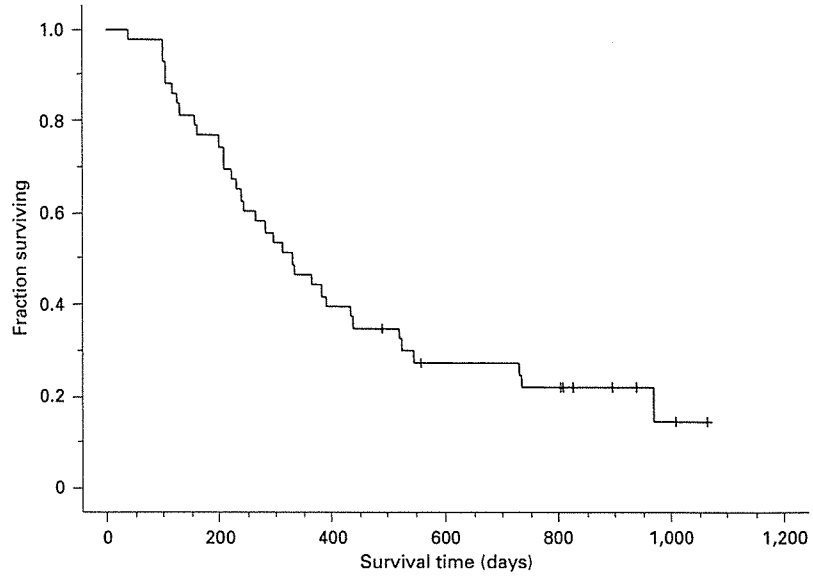

Fig. 1. Kaplan-Meier estimated overall survival curves. Median survival time was 47 weeks; 1-year survival rate was 47%.

Table 2. Chemotherapeutic evaluation (n = 43)

Cycles[1]	2 (1–4)
Response: CR/PR/NC/PD	1/20/20/2
Response rate, %	49
Response duration, weeks	
Average	39.2
Range	5–147
1-year survival rate, %	47

CR = Complete response; PR = partial response; NC = no change; PD = progressive disease.

[1]Value represents average with the range in parentheses.

Table 3. Toxicity (n = 43 patients)

	Maximum toxicity terms of CTC grade					Grade ≥3
	0	1	2	3	4	%
Leukopenia	1	1	6	29	6	81
Neutropenia	1	0	4	13	25	88
Anemia	1	6	18	18	–	42
Thrombocytopenia	25	5	7	6	0	14
Creatinine	23	18	1	1	0	2
SGOT/SGPT	30	12	1	0	0	0
Vomiting	5	7	31	0	–	0
Diarrhea	20	16	7	0	0	0
Alopecia	20	22	1	–	–	
Edema	36	6	1	0	–	0
Neuropathy	40	3	0	0	0	0

Figures represent number of patients. CTC = Common toxicity criteria; SGOT = serum glutamic oxaloacetic transaminase; SGPT = serum glutamic pyruvic transaminase.

Toxicity

Table 3 shows the types and grades of toxicities resulting from the treatment, using the common toxicity criteria. All 43 patients could be evaluated for toxic reactions. The major toxicity was myelosuppression. Leukopenia <2,000/mm^3 (grade 3 or 4) was observed in 35 patients (81%), of whom 6 patients showed grade 4. Neutropenia <1,000/mm^3 (grade 3 or 4) was observed in 38 patients (88%), of whom 25 patients showed grade 4. Eight patients developed febrile neutropenia. Thrombocytopenia <5 × 10^4/mm^3 (grade 3 or 4) was observed in 6 patients (14%), and a hemoglobin nadir (grade 3) in 18 patients (42%). There were no episodes of bleeding or fluid overload.

Vomiting grade ≥ 2 occurred in 31 patients (72%). Diarrhea grade ≥ 2 was observed in 7 patients (16%). Grade 1 or 2 alopecia and edema were observed in 23 and 7 patients, respectively. In the first cycle, creatinine showed grade ≥ 2 in 2 patients, resulting in transient rises. In the following cycle, the creatinine level was kept at grade 1 by reducing the dosage of cisplatin. Grade 1 or 2 skin rash was observed in 3 patients. Finally, there were no treatment-related deaths.

Discussion

Cisplatin is one of the key drugs for the treatment of NSCLC. Its high response rate of 40% and safety when it was given alone by continuous infusion over 5 days [14] are confirmed.

Docetaxel is also an active agent to treat NSCLC, and docetaxel of 60 mg/m^2/day (day 1), a recommended dose in Japan, showed a response rate of 19% [7]. Docetaxel has no cross-resistance with cisplatin, and in clinical practice, docetaxel was effective in some patients who were resistant to cisplatin [19]. In addition, additive effects are confirmed between cisplatin and docetaxel, and major side effects of the two drugs are different.

This was a phase II study to determine the usefulness and safety of combination chemotherapy of cisplatin (5-day continuous infusion) and docetaxel for the treatment of advanced NSCLC. The response rate in this study was 49%, which is higher than with docetaxel alone. In comparison with other combination therapies, response rates were 39–42% for cisplatin (bolus) and docetaxel [20, 21], and 58.5% for cisplatin (infusion) and irinotecan with G-CSF. In combination with cisplatin (bolus) and newly developed anticancer agents, the response rates were 44% with paclitaxel [22], 31% with gemcitabine [23], and 26% with vinorelbine [24]. Although these studies differed as regards patients' backgrounds, generally, combination therapies showed better response rates than docetaxel alone.

In our study, side effects predominantly involved hematological toxicity (leukopenia, neutropenia, and anemia). Fever associated with neutropenia was observed in 8 (23%) of 43 patients, and they were treated by administering antibiotics. Hematological toxicities were similar to those in other combination therapies [20, 21]. Nonhematological toxicities were mild, with only 1 patient showing an increased creatinine level of grade 3. The increase was transient, and soon returned to normal. Peripheral edema was observed in only 16%, which was markedly lower than the 24–46% found in other studies [5, 25, 26]. When accumulated doses of docetaxel exceeded 500 mg/m^2, the incidence of edema increased, and at a dose of 85 mg/m^2 or less, eruption was not observed [27]. The dosage was 60 mg/m^2 in our study, and no patients received 500 mg/m^2. There were no side effects concerning hypersensitivity or treatment-related deaths.

We carried out a phase II study of combination treatment of cisplatin (5-day continuous infusion) and docetaxel in 43 patients with NSCLC. The response rate was 49%, and median survival time was 47 weeks. A major side effect was neutropenia. A combination treatment of infusional cisplatin and docetaxel is a tolerable and active regimen for patients with advanced NSCLC. It is to be recommended as a candidate regimen in planning a phase III clinical study in advanced NSCLC, and this regimen will ultimately be evaluated in a phase III clinical study.

Acknowledgement

This work was supported in part by a grant-in-aid for cancer research from the Ministry of Health, Labour and Welfare (Tokyo, Japan), and by the Second Term Comprehensive 10-Year Strategy for Cancer Control.

References

1 Dillman RO, Seagren SL, Propert KJ, et al: A randomized trial of induction chemotherapy plus high-dose radiation versus radiation alone in stage III non-small-cell lung cancer. N Engl J Med 1990;323:940–945.
2 Rapp E, Pater JL, Willan A, et al: Chemotherapy can prolong survival in patients with advanced non-small cell lung cancer – Report of a Canadian multicenter randomized trial. J Clin Oncol 1988;6:633–641.
3 Pronzato P, Landucci M, Vaira A, Bertelli G: Carboplatin and etoposide as outpatient treatment of advanced non-small-cell lung cancer. Chemotherapy 1994;40:144–148.
4 Fossella FV, Lee JS, Murphy WK, et al: Phase II study of docetaxel for recurrent or metastatic non-small-cell lung cancer. J Clin Oncol 1994;12:1238–1244.
5 Francis PA, Rigas JR, Kris MG, et al: Phase II trial of docetaxel in patients with stage III and IV non-small-cell lung cancer. J Clin Oncol 1994;12:1232–1237.
6 Taguchi T, Furuse K, Niitani H, et al: Phase I clinical trial of RP 56976 (docetaxel), a new anticancer drug (in Japanese). Jpn J Cancer Chemother 1994;21:1997–2005.
7 Kunitoh H, Watanabe K, Onoshi T, et al: Phase II trial of docetaxel in previously untreated advanced non-small-cell lung cancer: A Japanese cooperative study. J Clin Oncol 1996; 14:1649–1655.

8 Ruckdeschel JC, Finkelstein DM, Mason BA, et al: Chemotherapy for metastatic non-small-cell bronchogenic carcinoma: EST 2575, generation V-A randomized comparison of four cisplatin-containing regimens. J Clin Oncol 1985;3:72–79.
9 Nakanishi Y, Takayama K, Wataya H, et al: Phase I study of weekly irinotecan combined with weekly cisplatin in patients with advanced solid tumors. Chemotherapy 2002;48:205–210.
10 Forastiere AA, Belliveau JF, Goren MP, et al: Pharmacokinetic and toxicity evaluation of five-day continuous infusion versus intermittent bolus *cis*-diamminedichloroplatinum (II) in head and neck cancer patients. Cancer Res 1988;48:3869–3874.
11 Drewinko B, Brown BW, Gottlieb JA: The effect of *cis*-diamminedichloroplatinum (II) on cultured human lymphoma cells and its therapeutic implications. Cancer Res 1973;33:3091–3095.
12 Matsushima Y, Kanzawa F, Hoshi A, et al: Time-schedule dependency of the inhibiting activity of various anticancer drugs in the clonogenic assay. Cancer Chemother Pharmacol 1985;14:104–107.
13 Belliveau JF, Posner MR, Ferrari L, et al: Cisplatin administered as a continuous 5-day infusion: Plasma platinum levels and urinary platinum excretion. Cancer Treat Rep 1986;70:1215–1217.
14 Saito Y, Mori K, Tominaga K, et al: Phase II study of 5-day continuous infusion of *cis*-diamminedichloroplatinum (II) in the treatment of non-small-cell lung cancer. Cancer Chemother Pharmacol 1990;26:389–392.
15 Mori K, Saito Y, Tominaga K, Yokoi K, Miyazawa N: Comparison of continuous and intermittent bolus infusions of metoclopramide during 5-day continuous intravenous infusion with cisplatin. Eur J Cancer 1991;27:729–732.
16 Mori K, Saito Y, Tominaga K: Antiemetic efficacy of alprazolam in the combination of metoclopramide plus methylprednisolone. Am J Clin Oncol 1993;16:338–341.
17 Mori K, Saito Y, Tominaga K: Phase II study of cisplatin continuous infusion plus vindesine in the treatment of non-small cell lung cancer. Am J Clin Oncol 1992;15:344–347.
18 Mori K, Machida S, Yoshida T, et al: A phase II study of irinotecan and infusional cisplatin with recombinant human granulocyte colony-stimulating factor support for advanced non-small-cell lung cancer. Cancer Chemother Pharmacol 1999;43:467–470.
19 Fossella FV, Lee JS, Shin DM, et al: Phase II study of docctaxel for advanced or metastatic platinum-refractory non-small-cell lung cancer. J Clin Oncol 1995;13:645–651.
20 Zalcberg J, Millward M, Bishop J, et al: Phase II study of docetaxel and cisplatin in advanced non-small-cell lung cancer. J Clin Oncol 1988;16:1948–1953.
21 Okamoto H, Watanabe K, Segawa Y, et al: Phase II study of docetaxel and cisplatin in patients with previously untreated metastatic non-small-cell lung cancer. Int J Clin Oncol 2000;5:316–322.
22 Giaccone G, Splinter AW, Debruyne C, et al: Randomized study of paclitaxel-cisplatin versus cisplatin-teniposide in patients with advanced non-small-cell lung cancer. J Clin Oncol 1998;16:2133–2141.
23 Sandler AB, Nemunaitis J, Denham C, et al: Phase III trial of gemcitabine plus cisplatin versus cisplatin alone in patients with locally advanced or metastatic non-small-cell lung cancer. J Clin Oncol 2000;18:122–130.
24 Wozniak AJ, Crowley JJ, Balcerzak SP, et al: Randomized trial comparing cisplatin with cisplatin plus vinorelbine in the treatment of advanced non-small-cell lung cancer: A Southwest Oncology Group Study. J Clin Oncol 1998;16:2459–2465.
25 Cerny T, Kaplan S, Pavlidis N, et al: Docetaxel (Taxotere) is active in non-small-cell lung cancer: A phase II trial of the EORTC early clinical trials group (ECTG). Br J Cancer 1994;70:384–387.
26 Miller VA, Rigas JR, Francis PA, et al: Phase II trial of a 75-mg/m^2 dose of docetaxel with prednisone premedication for patients with advanced non-small-cell lung cancer. Cancer 1995;75:968–972.
27 Extra JM, Rousseau F, Bruno R, et al: Phase I and pharmacokinetic study of Taxotere (RP 56976; NSC 628503) given as a short intravenous infusion. Cancer Res 1993;53:1037–1042.

Original Paper

Acta Haematologica

Acta Haematol 2006;115:78–90
DOI: 10.1159/000089471

Received: March 23, 2005
Accepted after revision: May 11, 2005

Histone Deacetylase Inhibitor Depsipeptide (FK228) Induces Apoptosis in Leukemic Cells by Facilitating Mitochondrial Translocation of Bax, Which Is Enhanced by the Proteasome Inhibitor Bortezomib

Krittaya Sutheesophon[a] Yukiko Kobayashi[a] Masa-aki Takatoku[b]
Keiya Ozawa[b] Yasuhiko Kano[c] Hideshi Ishii[a] Yusuke Furukawa[a,b]

[a]Division of Stem Cell Regulation, Center for Molecular Medicine, and [b]Division of Hematology, Department of Medicine, Jichi Medical School, and [c]Division of Medical Oncology, Tochigi Cancer Center, Tochigi, Japan

Key Words
Apoptosis · Bax · Histone deacetylase inhibitor · Leukemia · Mitochondria · Molecular-targeted therapy · Proteasome inhibitor

Abstract
Histone deacetylase (HDAC) inhibitors are promising candidates for molecular-targeted therapy for leukemia. In this study, we investigated the mechanisms of cytotoxic effects of depsipeptide (FK228), one of the most effective HDAC inhibitors against leukemia, using human myeloid leukemic cell lines HL-60 and K562. We found that FK228 activated caspase-9 and a subsequent caspase cascade by perturbing the mitochondrial membrane to release cytochrome *c*, which was almost completely blocked by overexpression of Bcl-2. The mitochondrial damage was caused by the translocation of Bax but not other pro-apoptotic Bcl-2 family proteins to the mitochondria. FK228 did not affect the interaction between Bax and Bax adaptor proteins such as 14-3-3θ and Ku70. FK228-induced apoptosis and mitochondrial translocation of Bax were markedly enhanced by the proteasome inhibitor bortezomib. The synergistic action of FK228 and bortezomib was at least partly mediated through conformational changes in Bax, which facilitate its translocation to the mitochondria. These results suggest that the combination of HDAC inhibitors and proteasome inhibitors is useful in the treatment of leukemia especially in the context of molecular-targeted therapy. The status of Bcl-2 and Bax may influence the sensitivity of tumors to this combination and thus can be a target of further therapeutic intervention.

Introduction

Because of the limited efficacy of conventional chemotherapy, the development of a novel treatment strategy is eagerly awaited for refractory and relapsed leukemias. Even among standard-risk patients with de novo acute myeloblastic leukemia (AML), only approximately 30% can achieve a long-term disease-free survival [1]. The treatment outcome is even worse in patients with high-risk AML, such as secondary leukemia, and in the elderly [2]. Most attempts to treat these patients with more intensive regimens have resulted in failure for two rea-

KARGER
Fax +41 61 306 12 34
E-Mail karger@karger.ch
www.karger.com

0001–5792/06/1152–0078$23.50/0

Accessible online at:
www.karger.com/aha

Yusuke Furukawa, MD
Division of Stem Cell Regulation, Center for Molecular Medicine
Jichi Medical School, 3311-1 Yakushiji, Minamikachi-machi
Tochigi 329-0498 (Japan)
Tel. +81 285 58 7400, Fax +81 285 44 7501, E-Mail furuyu@jichi.ac.jp

sons. First, the leukemic cells of these patients are no longer responsive to cytotoxic drugs with a conventional mode of action such as DNA alkylation or inhibition of DNA synthesis. Second, intensive treatment often causes serious side effects including severe myelosuppression in elderly and/or previously treated patients. In order to improve the prognosis of these patients, the establishment of molecular-targeted therapy, which involves therapeutic agents with different mechanisms of action and high specificity, is highly anticipated. Among the newly developed drugs, histone deacetylase (HDAC) inhibitors and proteasome inhibitors are two promising candidates for molecular-targeted therapy against refractory and relapsed leukemias.

Recently, small compounds that inhibit HDAC activity have become available as a tool for cancer treatment [3]. These compounds, collectively referred to as HDAC inhibitors, restore the expression of genes aberrantly silenced in cancer cells by reversing HDAC-mediated deacetylation of their promoter regions and transcriptional repression. In addition to core histones at gene promoters, HDAC inhibitors also acetylate several cellular proteins such as p53 and E2F-1 and modify their functions [4, 5]. As a sum of these effects, HDAC inhibitors induce cell cycle arrest, differentiation, and apoptosis in cancer cells, all of which have been demonstrated in numerous preclinical studies [6]. Given that the tethering of HDACs to promoters of genes regulating cell differentiation and growth control is commonly observed in leukemias, especially in those having leukemic fusion proteins [7], HDAC inhibitors fulfill the requirement of molecular-targeted therapy for refractory and relapsed leukemias. Currently, phase I and II clinical trials are ongoing for five different types of HDAC inhibitors – sodium phenylbutyrate, valproic acid, depsipeptide (FK228), suberoylanilide hydroxamic acid, and MS-275 – in hematologic malignancies [8]. Depsipeptide (FK228) is especially promising, because it shows considerable activity against T-cell lymphoma, AML, and chronic lymphocytic leukemia [9, 10]. For a safe and effective clinical application, however, it is essential to clarify the molecular basis of the cytotoxic activity of this drug. Unfortunately, relatively little is known about the mechanisms of the cytotoxic effect of depsipeptide (FK228) in leukemias compared with those in solid tumors.

Recently, targeting the ubiquitin-proteasome pathway has emerged as a novel approach for cancer treatment. The proteasome is an essential enzyme complex that catalyzes the degradation of a variety of short-lived functional proteins with ubiquitination as a marker [11]. This system is indispensable for the elimination of impaired proteins arising from oxidative stress, heat shock, and transcription of mutant genes, and plays an important role in the regulation of many biological processes such as cytokine-mediated transcription, cell cycle progression, and apoptosis [12]. For unknown reasons, inhibition of the ubiquitin-proteasome pathway induces growth arrest and apoptosis preferentially in cancer cells, which constitutes a rationale for the usage of proteasome inhibitors in cancer treatment [13]. Bortezomib (Velcade®, formerly known as PS-341) is the sole proteasome inhibitor whose anti-tumor activity has been confirmed in both preclinical experiments and clinical trials [14]. This drug was recently approved for use in patients with refractory and relapsed multiple myeloma, and will be applied for the treatment of other hematologic malignancies and solid tumors in the near future [15]. Because bortezomib is known to enhance the sensitivity of tumor cells to various anti-cancer drugs [16], bortezomib and depsipeptide (FK228) may be the best combination for molecular-targeted therapy in leukemias.

In this study, we investigated the mechanisms of FK228-induced apoptosis in leukemic cells, and found that FK228 activated the mitochondrial pathway of apoptosis via mitochondrial translocation of Bax, a pro-apoptotic Bcl-2 family protein, which was enhanced by bortezomib. This finding is useful for safe and effective clinical applications of the two drugs in the near future.

Materials and Methods

Reagents

All chemicals were purchased from Sigma (St. Louis, Mo., USA) unless otherwise stated. Depsipeptide (FK228) and bortezomib (Velcade) were provided by Fujisawa (Osaka, Japan) and Millennium Pharmaceuticals (Cambridge, Mass., USA), respectively. Cell-permeable fluoromethylketone-derivatized peptides corresponding to specific binding sites for caspases were used as caspase inhibitors (R & D Systems, Minneapolis, Minn., USA). Stock solutions were made with dimethylsulfoxide (DMSO) at 10 m*M* and used at a final concentration of 100 μ*M* in growth medium (final DMSO concentration was 1%). A colorimetric assay kit for caspase-9 was also obtained from R & D Systems.

Cells and Cell Culture

Human myeloid leukemia cell lines HL-60 and K562 were purchased from the American Type Culture Collection (Manassas, Va., USA). HL-60 and K562 stable transformants constitutively overexpressing Bcl-2 (HL-60/Bcl-2 and K562/Bcl-2) and their controls carrying an empty vector (HL-60/mock and K562/mock) were established in our laboratory as previously reported [17, 18]. These cell lines were maintained in RPMI1640 medium supplemented

with 10% fetal bovine serum according to the manual provided by the American Type Culture Collection.

Flow Cytometry

The cell cycle profile was obtained by staining DNA with propidium iodide in preparation for flow cytometry with the FACScan/CellQuest system (Becton-Dickinson, San Jose, Calif., USA). The size of the sub-G1, G0/G1, and S+G2/M fractions was calculated as a percentage by analyzing DNA histograms with the ModFitLT 2.0 program (Verity Software, Topsham, Maine, USA).

Measurement of the Mitochondrial Transmembrane Potential

The mitochondrial transmembrane potential was measured with a MitoCapture Mitochondrial Apoptosis Detection Kit (Medical & Biological Laboratories, Nagoya, Japan). MitoCapture® is a rhodamine derivative that aggregates in the mitochondria and generates a bright red fluorescence in intact cells. The intensity of the red fluorescent signal (FL2-H on flow cytometry) diminishes as the mitochondrial membrane is perturbed.

Western Blotting

Immunoblotting was carried out according to the standard method using the following antibodies: anti-procaspase-9 (68086E; BD Biosciences Pharmingen, San Jose, Calif., USA), anti-cleaved caspase-9 (9501; Cell Signaling Technology, Beverly, Mass., USA), anti-procaspase-6 (B93-4; BD Biosciences Pharmingen), anti-procaspase-3 (clone 97; BD Transduction Laboratories, Lexington, Ky., USA), anti-cleaved caspase-3 (9661; Cell Signaling Technology), anti-caspase-7 (B94-1; BD Biosciences Pharmingen), anti-Bcl-2 (clone 7; BD Transduction Laboratories), anti-Bax (2772; Cell Signaling Technology, clone 3; BD Transduction Laboratories, 554104; BD Biosciences Pharmingen), anti-Bak (3792), anti-Bid (2002), anti-Bad (9292; all Cell Signaling Technology), anti-14-3-3θ (C23-1; BD Biosciences Pharmingen, C-17; Santa Cruz Biotechnology), anti-Ku70 (clone 15; BD Transduction Laboratories), anti-ASC/TMS1 (D14885; Calbiochem-Novabiochem, San Diego, Calif., USA) and anti-β-actin (C4; ICN Biomedicals, Aurora, Ohio, USA). To detect conformational changes of Bax, we prepared protein samples using CHAPS cell extract buffer (Cell Signaling Technology) as previously described [19].

Confocal Laser Microscopy

Cells were collected on glass slides using a Cytospin centrifugator (Shandon Scientific, Runcorn, UK), and fixed in 4% paraformaldehyde in phosphate-buffered saline. In situ staining for cytochrome *c* was carried out using anti-cytochrome *c* monoclonal antibody (6H2.B4; Pharmingen) and Alexa-488-conjugated antibody to mouse immunoglobulin (Molecular Probes, Eugene, Oreg., USA) as primary and secondary antibodies, respectively [20]. For co-labeling of mitochondria, we used a rabbit polyclonal antibody against 62-kDa mitochondrial protein (AB3598; Chemicon International, Temecula, Calif., USA) and Cy3-conjugated goat antibody to rabbit immunoglobulin (Amersham Pharmacia Biotech, Piscataway, N.J., USA) as primary and secondary antibodies, respectively. In situ staining for Bax was performed similarly using anti-Bax (554104, BD Biosciences Pharmingen, or N-20, Santa Cruz Biotechnology) and anti-human mitochondria (AE-1; Leinco Technologies, St. Louis, Mo., USA) antibodies.

Table 1. Effects of caspase inhibitors on FK228-induced apoptosis

Additions	Targets	Sub-G1 fractions, %[a]	p values[b]
DMSO	–	74.1 ± 10.6	
Z-VAD-fmk	general	38.2 ± 8.2	0.00482117
Z-WEHD-fmk	caspase-1	87.5 ± 5.9	0.06434876
Z-VDVAD-fmk	caspase-2	76.7 ± 8.5	0.37702580
Z-DEVD-fmk	caspase-3	76.0 ± 7.8	0.40574888
Z-YVAD-fmk	caspase-4	77.0 ± 9.9	0.37333352
Z-VEID-fmk	caspase-6	78.6 ± 12.5	0.32866905
Z-LETD-fmk	caspase-8	81.3 ± 11.0	0.22898378
Z-LEHD-fmk	caspase-9	22.7 ± 9.4	0.00165079
Z-AEVD-fmk	caspase-10	78.8 ± 13.5	0.32972531
Z-LEED-fmk	caspase-13	78.6 ± 9.7	0.30780867

[a] Means ± SD of three independent experiments.
[b] p values against the DMSO control were determined by an unpaired Student's t test.

Results

Involvement of a Caspase-9-Initiated Caspase Cascade in FK228-Induced Apoptosis

When HL-60 and K562 myeloid leukemia cell lines were treated with depsipeptide (FK228) at 20 n*M* (approximately 1/50 of the mean maximal plasma concentration determined in phase I clinical trials [21]), approximately 75% of cells underwent apoptosis as judged by the size of sub-G1 fractions on DNA histograms (fig. 1a, DMSO) and annexin V staining (data not shown) after 48 h of culture. To determine the pathways of apoptotic signal transduction activated by FK228, we examined the effects of caspase inhibitors on FK228-induced apoptosis. HL-60 cells were pre-treated with cell-permeable caspase-binding peptides, and then cultured in the presence of 20 n*M* FK228. The percentage of cells undergoing apoptosis was measured by calculating sub-G1 fractions on DNA histograms after 48 h. A representative result is shown in figure 1a, and the results of three independent experiments are summarized in table 1. The size of sub-G1 fractions was significantly ($p < 0.01$) decreased by a general caspase inhibitor (VAD) as well as a specific inhibitor for caspases-9 (LEHD), suggesting a pivotal role for caspase-9 in the FK228-induced apoptosis of HL-60 cells. We obtained similar results in experiments using K562 cells, except that K562 was relatively insensitive to FK228 compared with HL-60 (data not shown).

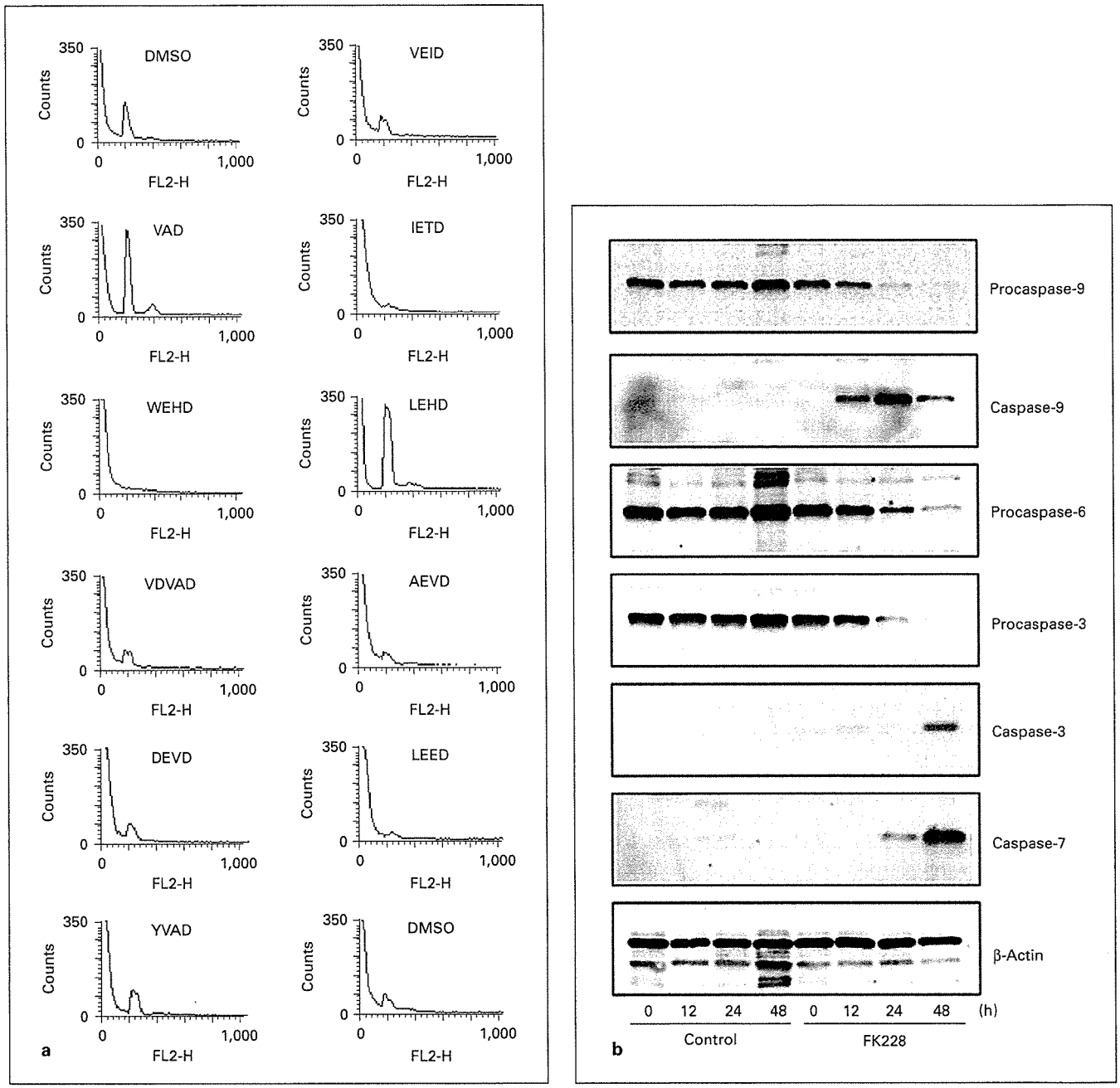

Fig. 1. Involvement of a caspases-9-initiated caspase cascade in FK228-induced apoptosis. **a** HL-60 cells were seeded at 5×10^5 cells/ml with various caspase inhibitors (100 μ*M* final) or DMSO (solvent), and cultured in the presence of 20 n*M* FK228. After 48 h, the cells were harvested and subjected to a flow-cytometric analysis to obtain the cell cycle profile. The size of the sub-G1 fractions was calculated and summarized in table 1. **b** HL-60 cells were cultured in the absence (control) or presence (FK228) of 20 n*M* FK228. Whole-cell lysates were prepared at given time points, and subjected to immunoblot analysis for the expression of caspases. The membranes were reprobed with anti-β-actin antibody to verify the equal loading and integrity of samples. Data shown are representative of multiple independent experiments.

To confirm the activation of caspase-9 during FK228-mediated apoptosis, we examined the expression and cleavage of caspases in HL-60 cells cultured with FK228 for up to 48 h by immunoblotting. As shown in figure 1b, the amount of procaspase-9 (47 kDa) decreased after 12 h of culture with an active cleaved fragment of caspase-9 (17 kDa) appearing in a reciprocal manner. We simultaneously measured the enzymatic activity of caspase-9 using a colorimetric assay kit, and confirmed that it indeed increased in FK228-treated cells in accord with the processing of procaspase-9 (data not shown). With slightly delayed kinetics, procaspase-6 (35 kDa) and procaspase-3 (35 kDa) were processed into a large active subunit (17 kDa) in these cells. In addition, an active fragment of caspase-7 (20 kDa) appeared after 24 h. These results support the notion that FK228 activates caspase-9, which in turn processes caspases-6, -3 and -7 to initiate a caspase cascade, leading to apoptotic cell death in myeloid leukemic cells.

FK228 Activates Caspase-9 via Mitochondrial Pathways

When mitochondria are damaged by certain apoptotic stimuli such as ionizing radiation and anti-cancer drug treatment, cytochrome *c* is released from the mitochondria into the cytosol, where it triggers the activation of caspase-9 [22]. We therefore examined whether FK228 induced the disruption of the mitochondrial membrane and cytoplasmic translocation of cytochrome *c* in HL-60 cells. As shown in figure 2a, the mitochondrial transmembrane potential was apparently decreased by FK228 after 12 h of treatment (the results of three independent ex-

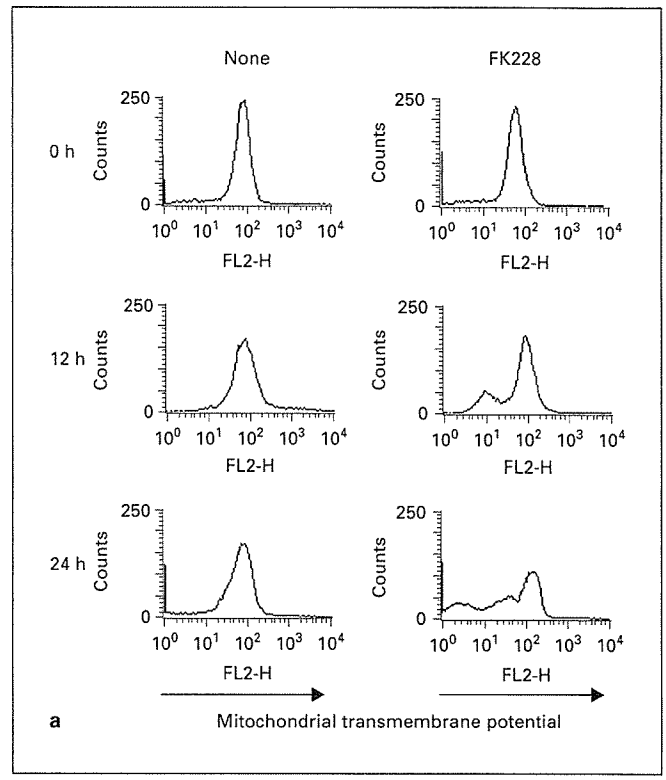

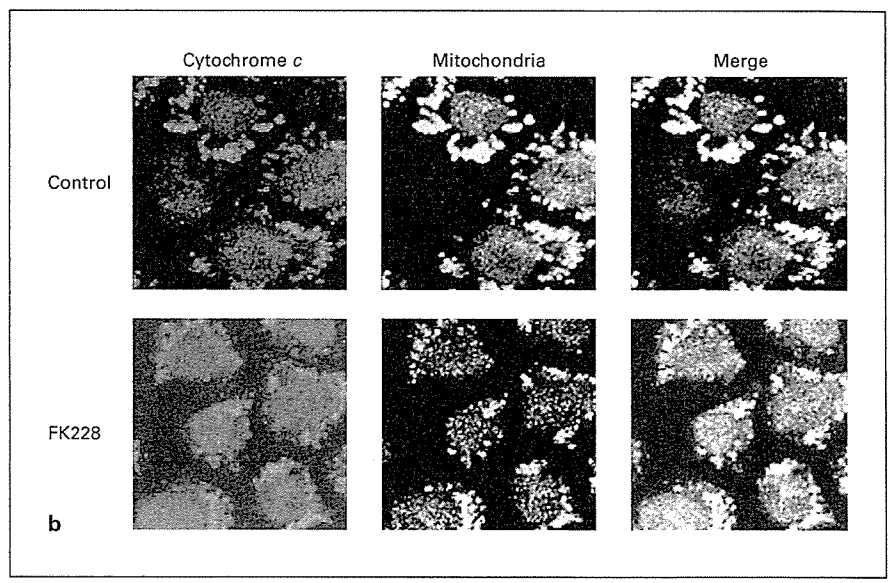

Fig. 2. FK228 induces apoptosis via mitochondrial pathways. **a** HL-60 cells were cultured in the absence (none) or presence of 20 n*M* depsipeptide (FK228) for 12 and 24 h, and stained with a MitoCapture dye to measure the mitochondrial transmembrane potential (FL2 signal). The results of three independent experiments are summarized in table 2. **b** After 24 h of culture, cells were double-stained with anti-cytochrome *c* and anti-mitochondrial protein antibodies, and examined under a confocal laser microscope. Data shown are representative of multiple independent experiments.

periments are summarized in table 2). Next, we examined the intracellular distribution of cytochrome *c* using confocal laser microscopy. In untreated HL-60 cells, cytochrome *c* was stained in a perinuclear punctate pattern indicative of intra-mitochondrial localization, which was confirmed by co-labeling with mitochondrial markers (fig. 2b, control). During apoptosis triggered by FK228, the distribution of cytochrome *c* became completely diffuse, reflecting the release of cytochrome *c* from the damaged mitochondria into the cytosol (fig. 2b, FK228).

To further confirm the involvement of mitochondrial damage in FK228-induced apoptosis, we investigated whether Bcl-2, a major protector of the mitochondrial membrane, could suppress the effect of FK228 on leukemic cells. For this purpose, we established HL-60 and K562 sublines, HL-60/Bcl-2 and K562/Bcl-2, which constitutively overexpress Bcl-2. Using immunoblotting, we confirmed that both cell lines expressed Bcl-2 protein at levels approximately 10-fold higher than their mock-transfected controls (fig. 3a). Bcl-2 overexpression

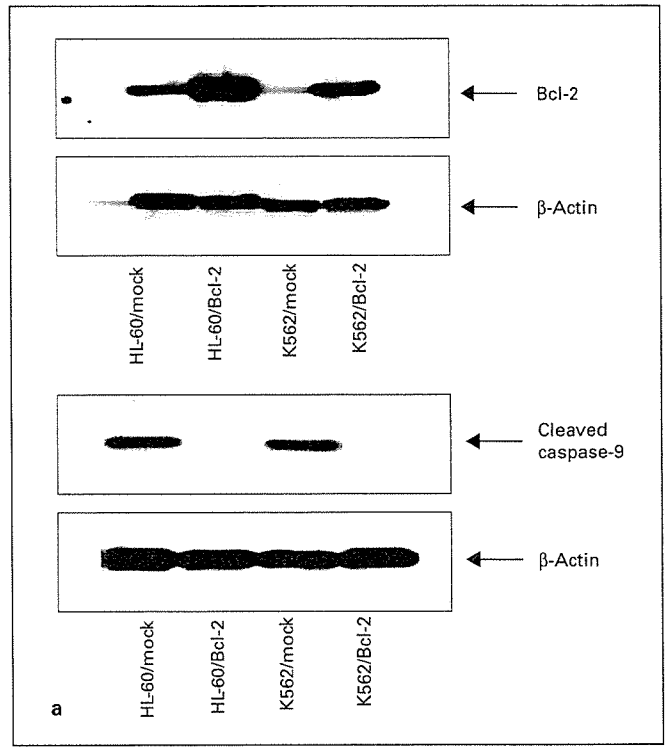

Table 2. Mitochondrial transmembrane potential of FK228-treated HL-60 cells

Time in culture	Mean fluorescence intensities[a]		p values[b]
	control	FK228 treated	
0 h	83.2 ± 5.8	81.4 ± 5.0	0.40049790
12 h	70.7 ± 2.1	45.1 ± 12.9	0.04196319
24 h	71.0 ± 10.5	17.1 ± 6.7	0.00523239

[a] Means ± SD of three independent experiments.
[b] p values determined by a paired Student's t test between the data of control and FK228-treated cells.

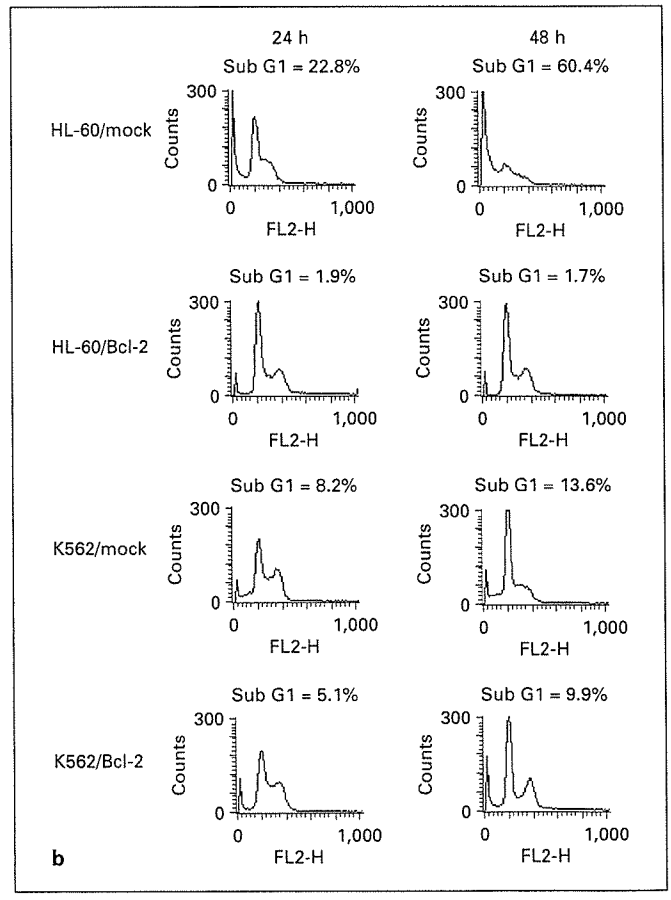

Fig. 3. Bcl-2 overexpression inhibits FK228-mediated activation of caspase-9 and apoptosis in HL-60 and K562 cells. We cultured Bcl-2-overexpressing HL-60 and K562 sublines (HL-60/Bcl-2 and K562/Bcl-2) and their mock-transfected controls (HL-60/mock and K562/mock) in medium containing 20 n*M* FK228. **a** Immunoblot analysis for Bcl-2 and cleaved caspase-9 was carried out after 24 h. β-Actin was used as a loading control. Data shown are representative of multiple independent experiments. **b** Cells were harvested at the indicated time points and subjected to a flow-cytometric analysis to obtain the cell cycle profile. The size of the sub-G1 fraction was calculated with the ModFitLT 2.0 program. The results of three independent experiments are summarized in table 3.

almost completely blocked the FK228-induced activation of caspase-9 (fig. 3a), loss of mitochondrial transmembrane potential (data not shown), and apoptotic cell death (fig. 3b, table 3) in both HL-60 and K562 cells. It is of note that the inhibitory effect was less striking in K562 probably due to its relative resistance to this drug, although the effect of Bcl-2 was statistically significant (table 3).

FK228 Facilitates the Translocation of Bax from the Cytosol to the Mitochondria

Next, we investigated the mechanisms by which FK228 perturbed the mitochondrial membrane to initiate caspase-9-triggered signaling pathways of apoptosis. It is well known that the integrity of the mitochondrial membrane is regulated by the balance between pro- and anti-apoptotic members of the Bcl-2 family [23]. The former include multidomain pro-apoptotics (Bax and Bak) and BH3-only proteins (Bid, Bad, Bim, and Noxa), whereas major examples of the latter are Bcl-2 and Bcl-x. In a steady-state, anti-apoptotic Bcl-2 family proteins reside in the outer mitochondrial membrane and suppress the release of cytochrome *c*. Following a variety of death signals, pro-apoptotic Bcl-2 family members undergo post-translational modifications, such as conformational changes and cleavage, and translocate from the cytosol to the mitochondria, where they stimulate the release of cytochrome *c* by directly affecting the mitochondrial membrane and/or inhibiting the activity of anti-apoptotic Bcl-2 proteins. With this background in mind, we examined the expression profile of Bcl-2 family proteins in FK228-treated HL-60 cells using immunoblotting. Among pro-apoptotic family members, Bax, Bak, and Bid but not Bad, Bim, and Noxa were expressed in HL-60 (fig. 4a) [18, and data not shown]. Bcl-2 but not Bcl-x was present in HL-60 cells as a protector of mitochondria (fig. 4a) [18]. FK228 neither affected the abundance of Bax, Bak, Bid, and Bcl-2 proteins, nor induced the cleavage of Bid in HL-60 cells (fig. 4a).

We then examined the intracellular distribution of pro-apoptotic Bcl-2 proteins by confocal laser microscopy. As shown in figure 4b, translocation of Bax from the cytosol to the mitochondria was observed in FK228-treated cells, whereas no changes in the distribution of Bid and Bak were found (data not shown). It has been reported that the translocation of Bax is regulated by two mechanisms: an interaction with adaptor proteins [24–26] and conformational changes [27]. We hypothesized that FK228 disrupted the association of Bax with adaptor proteins by acetylating Bax and/or Bax adaptors. To test this, Bax-containing protein complexes were immunoprecipitated from untreated and FK228-treated HL-60 cells, and subjected to immunoblotting with specific antibodies against known adaptor proteins for Bax: 14-3-3θ, Ku70, and ASC. As shown in figure 4c, FK228 did not affect the association of Bax with 14-3-3θ and Ku70, and Bax did not form a complex with ASC in HL-60 cells. In addition, we could not detect the acetylation of Bax protein in HL-60 cells even after FK228 treatment (data not shown). After negating the involvement of Bax-adaptor protein interaction, we focused on the conformational changes as a possible cause of the FK228-mediated translocation of Bax to the mitochondria.

Table 3. Effects of Bcl-2 overexpression on FK228-induced apoptosis

Cell lines	Time in culture, h	Sub-G1 fractions, %[a]		p values[b]
		mock	Bcl-2	
HL-60	24	20.9 ± 2.3	1.9 ± 5.0	0.00283877
	48	70.7 ± 9.4	3.2 ± 1.3	0.00552666
K562	24	8.6 ± 2.9	5.0 ± 0.2	0.04001607
	48	22.8 ± 8.4	9.1 ± 1.5	0.03833046

[a] Means ± SD of three independent experiments.
[b] p values determined by a paired Student's t test between the data from mock-transfected cells and Bcl-2-overexpressing cells.

Synergistic Effects of FK228 and Bortezomib on Apoptosis and Translocation of Bax to the Mitochondria

Taking into account a report that proteasome inhibitors induce conformational changes and mitochondrial translocation of Bax in chronic lymphocytic leukemia cells [28], we investigated whether proteasome inhibitors could enhance the effects of FK228 on the intracellular distribution of Bax and cell viability in myeloid leukemic cells. We chose bortezomib (Velcade) as a proteasome inhibitor because of its known efficacy against leukemias in vitro and in vivo [29]. As shown in figure 5a, bortezomib did not induce apoptosis in HL-60 cells after 24 h of culture at a concentration of 50 n*M*, approximately 1/30 of the mean maximal plasma concentration determined in phase I clinical trials [30]. FK228 only slightly affected cell viability at a suboptimal concentration (2 n*M*), where-

as it caused cell cycle arrest at both G1 and G2 phases. As anticipated, the apoptosis-inducing effect of FK228 was dramatically augmented by bortezomib; almost all cells underwent apoptosis in the presence of 2 n*M* FK228 and 50 n*M* bortezomib (a representative result is shown in figure 5a, and the results of three independent experiments are summarized in table 4). Importantly, the syn-

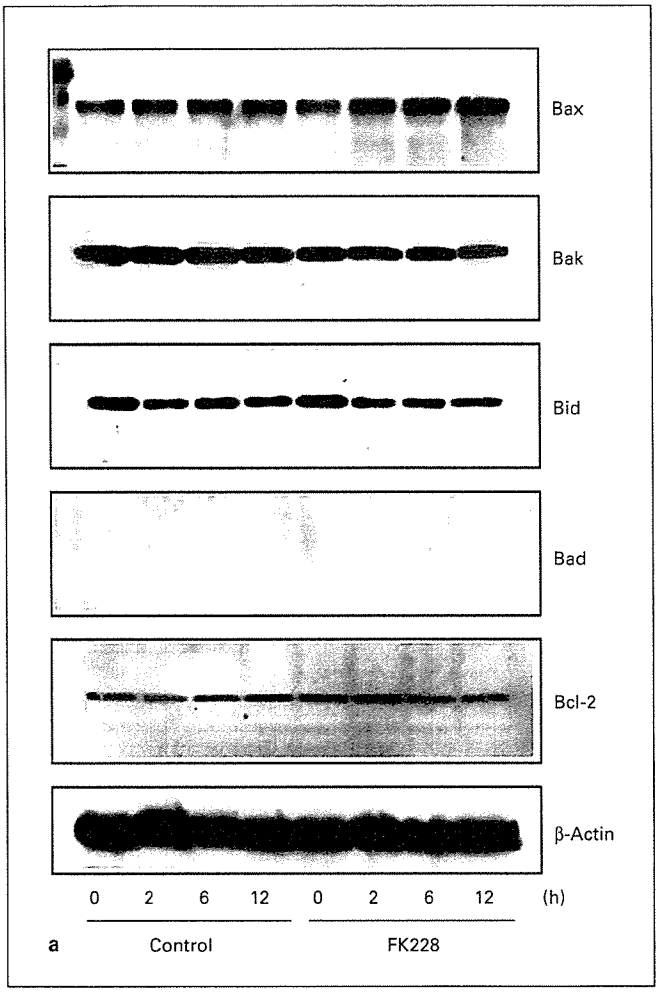

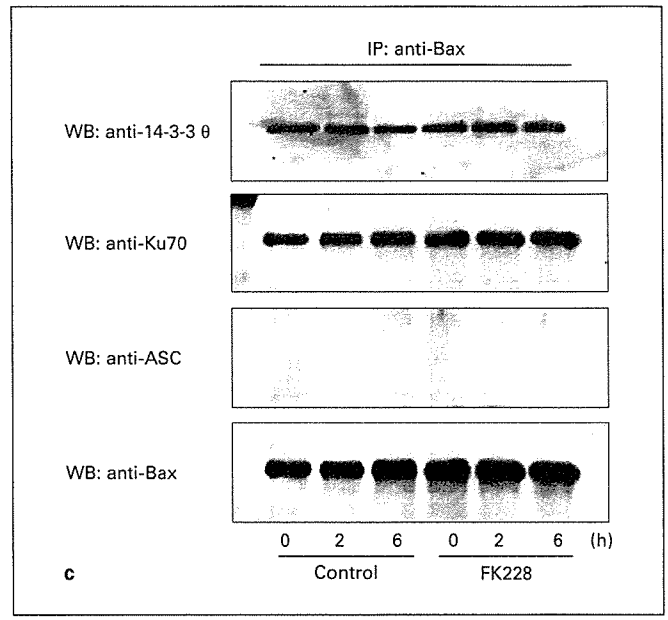

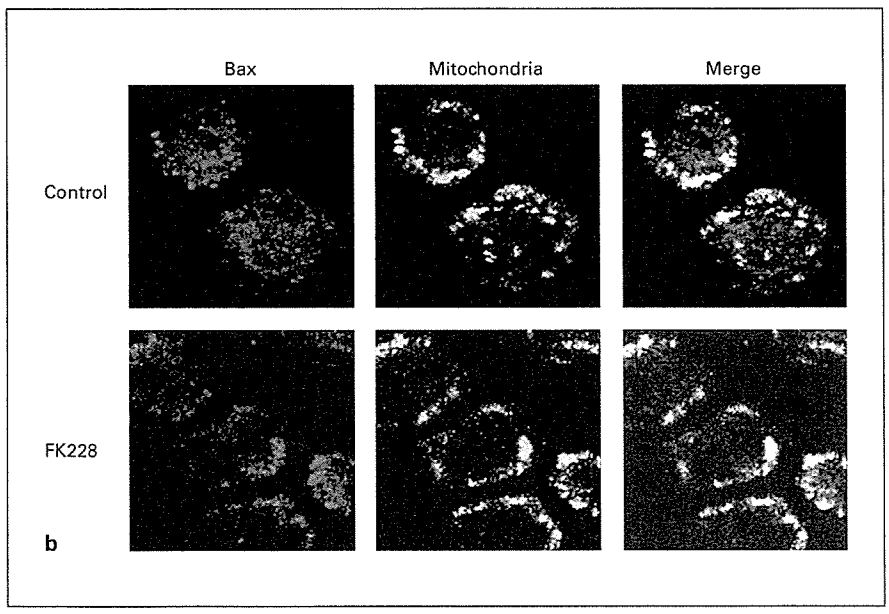

Fig. 4. Role of Bcl-2 family proteins in FK228-induced apoptosis. HL-60 cells were cultured in the absence (control) or presence (FK228) of 20 n*M* FK228. **a** Whole-cell lysates were isolated at given time points and subjected to immunoblot analysis for Bcl-2 family proteins as indicated. **b** After 24 h, cells were double-stained with anti-Bax and anti-mitochondria antibodies, and analyzed by confocal laser microscopy. **c** Bax-containing complexes were immunoprecipitated at the indicated time points using rabbit polyclonal antibody against Bax (2772), followed by immunoblotting using mouse monoclonal antibodies against 14-3-3θ, Ku70, and ASC. The membranes were reprobed with mouse monoclonal anti-Bax antibody (clone 3) to confirm the equal efficiency of immunoprecipitation. Data shown are representative of multiple independent experiments. WB = Western blotting; IP = immunoprecipitation.

ergistic induction of apoptosis was not observed in Bcl-2-overexpressing HL-60 sublines (data not shown), suggesting that the two drugs share a common pathway.

Next, we performed a confocal microscopic analysis to evaluate the synergistic effects of the two drugs on the intracellular distribution of Bax. Neither FK228 nor bortezomib alone caused the translocation of Bax to the mitochondria at suboptimal concentrations (2 and 50 n*M*, respectively) and early time points (6 h; fig. 5b). In striking contrast, Bax was prominently accumulated in the mitochondria in the presence of both drugs even under the suboptimal condition (fig. 5b, FK228 + Velcade). These results clearly indicate that bortezomib enhances FK228-induced mitochondrial translocation of Bax and subsequent activation of the mitochondrial pathway of apoptosis.

Finally, we investigated the molecular basis of the synergistic enhancement of Bax translocation. To this end, we examined the conformational changes of Bax using antibodies that specifically recognize Bax in open configuration (clone 3 and N-20; fig. 5c shows the results of the experiments using clone 3) [31]. We simultaneously used the antibody 554104, which can detect Bax regardless of its configuration [27, 31], to estimate the total amount of Bax. As shown in figure 5c, bortezomib readily increased the amount of conformationally changed Bax, whereas the effect of FK228 alone was only marginal. Remarkably, the conformational change of Bax was further augmented by the combination of the two drugs. These results suggest that the synergistic effect of FK228 and bortezomib is at least in part mediated through conformational changes of Bax.

Table 4. Synergistic effects of FK228 and bortezomib on HL-60 cells

Additions	Sub-G1 fractions, %[a]	p values[b]
None	1.5 ± 0.4	0.00074174
FK228	10.6 ± 2.0	0.00116430
Velcade	2.6 ± 1.1	0.00078105
FK228 + Velcade	90.6 ± 5.9	

[a] Means ± SD of three independent experiments.
[b] p values determined by a paired Student's t test against the data from cells treated with both FK228 and bortezomib (Velcade).

Discussion

HDAC inhibitors are emerging as a novel class of anticancer reagents [3, 8]. Because of their unique mechanisms of action, HDAC inhibitors are expected to be effective against tumors resistant to conventional chemotherapy. According to recent results of phase I and II clinical studies, however, the effect of HDAC inhibitors

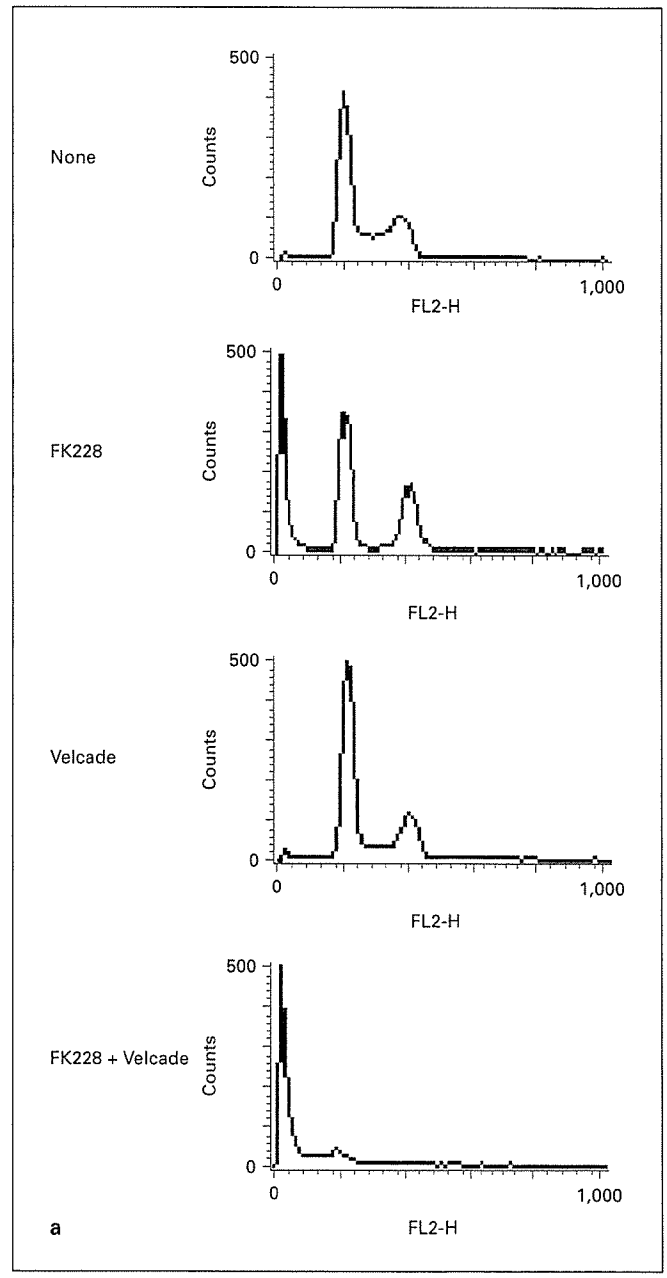

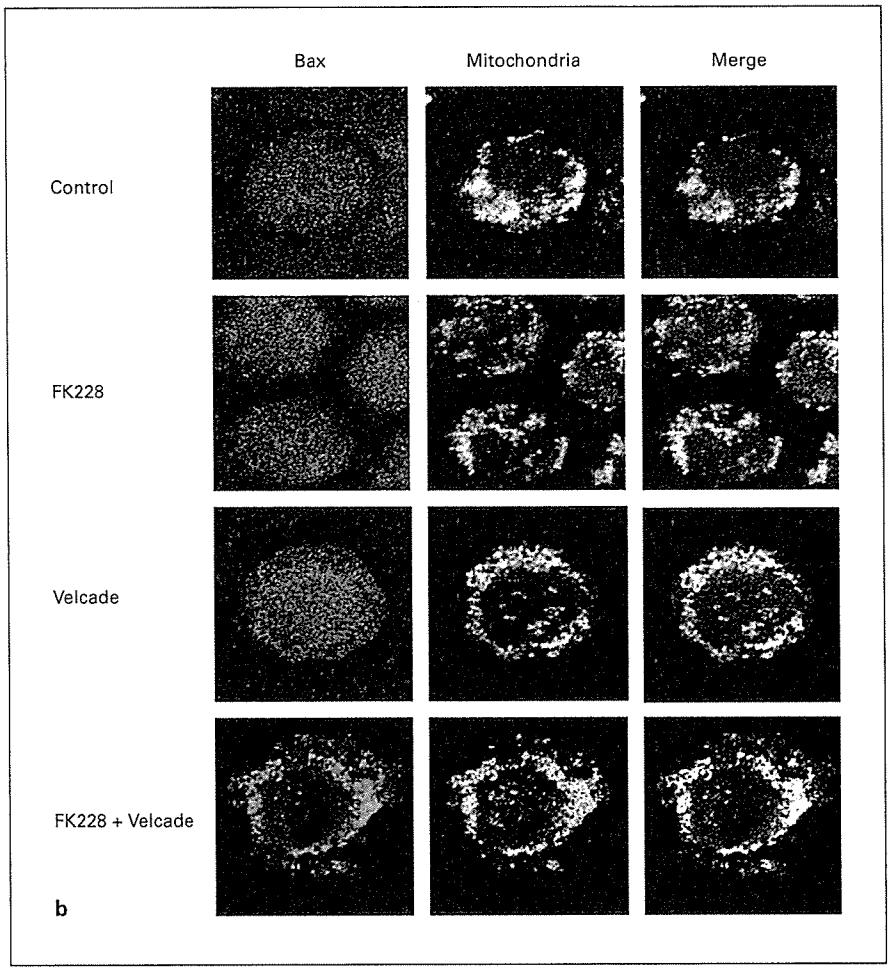

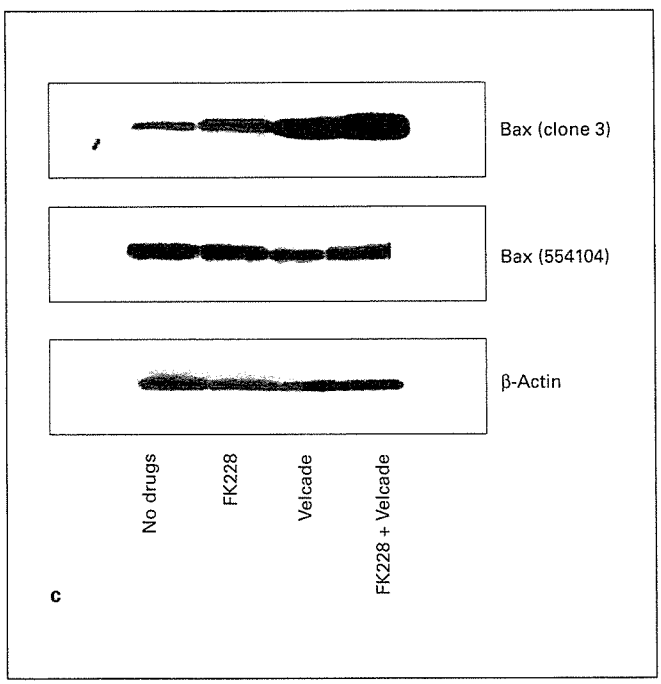

Fig. 5. Synergistic effects of FK228 and bortezomib on apoptosis and mitochondrial translocation of Bax. **a** HL-60 cells were cultured in the absence (none) or presence of either 2 n*M* FK228, 50 n*M* bortezomib (Velcade), or 2 n*M* FK228 and 50 n*M* bortezomib for 24 h, and subjected to cell cycle analysis. The size of the sub-G1 fractions was calculated and summarized in table 4. **b** HL-60 cells were cultured as above, and double-stained with antibodies against Bax and human mitochondria after 6 h. **c** Whole-cell lysates were prepared in CHAPS cell extract buffer after 24 h of culture, and subjected to immunoblotting with an antibody that specifically recognizes conformationally altered Bax (clone 3), conformation-independent Bax antibody (554104), and anti-β-actin antibody. Data shown are representative of multiple independent experiments.